ISBN: 978-3-95450-238-7 ISSN: 2226-0358 doi:10.18429/JACoW-ICALEPCS2023-TUPDP006

SYSTEM IDENTIFICATION EMBEDDED IN A HARDWARE-BASED CONTROL SYSTEM WITH CompactRIO*

T. R. S. Soares†, J. P. S. Furtado, V. B. Falchetto, G. O. Brunheira, J. L. B. Neto, R. R. Geraldes
Brazilian Synchrotron Light Laboratory, CNPEM, Campinas, Brazil

Abstract

The development of innovative model-based design high bandwidth mechatronic systems with stringent performance specifications has become ubiquitous at LNLS-Sirius beamlines. To achieve such unprecedented specifications, closed loop control architecture must be implemented in a fast, flexible, and reliable platform such as NI's CompactRIO (cRIO) controller that combines FPGA and real-time capabilities. The design phase and life-cycle management of such mechatronics systems heavily depends on high quality experimental data either to enable rapid prototyping, or even to implement continuous improvement process during operation. This work aims to present and compare different techniques to stimulus signal generation approaching Schröder phasing and Tukey windowing for better crest factor, signal-to-noise ratio, minimum mechatronic stress, and plant identification. Also shows the LabVIEW implementation that requires specific signal synchronization and processing on the main application containing a hardware-based control architecture, increasing system diagnostic and maintenance ability. Finally, experimental results from the High-Dynamic Double-Crystal Monochromator (HD-DCM-Lite) of QUATI (quick absorption spectroscopy) and SAPUCAIA (small-angle scattering) beamlines and from the High-Dynamic Cryogenic Sample Stage (HD-CSS) from SAPOTI (multi-analytical X-ray tech-nique) of CARNAÚBA beamline are also presented in this paper.

INTRODUCTION

System identification is the initial process of Model-Based Control Design (MBD), that builds a mathematical model representing the behavior of a system based on measurements of stimulus and response signals. In LNLS-Sirius [1], for the High-Dynamic Double-Crystal Monochromators (HD-DCM-Lite) [2, 3] and High-Dynamic Cryogenic Sample (HD-CSS) Stage, system identification in the frequency domain is the first step followed by controller design based in the loop shaping technique [4], controller embedding and validation. A good system identification provides accurate models, allows reliable controller design and one of its critical aspects is the stimulus signal, that requires specific characteristics mentioned later in this article. Also, all signal paths should be the same as seen by the control system, ensuring every component is included in the identified system, with simultaneous sampling of stimulus and response signals.

In order to increase system diagnostic and validation capabilities, stimulus generation and acquisition of system response were embedded alongside the hardware-based control algorithm, which required few modifications given the integration flexibility of the cRIO [5], highly customized with LabVIEW Real-Time and LabVIEW FPGA. Acquired signals are post-processed in MATLAB to estimate frequency response of the system.

ARCHITECTURE

HD-DCM-Lite and HD-CSS share a common high dynamic control architecture, presented in Fig. 1, where the controller, kinematics (homogeneous) transformations, and mechanical structure are specific for each application.

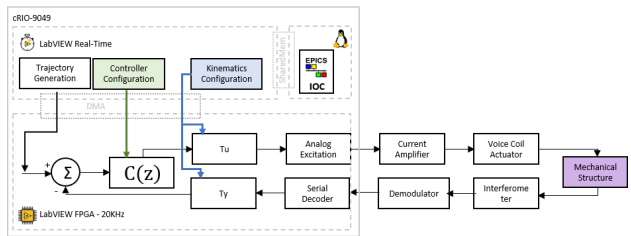

Figure 1: Common high dynamic control architecture.

The stimulus generation and response acquisition blocks were added in the Real-Time code to save FPGA resources, thus the FPGA works as a streaming bridge between the excitation signal generation (in Real-Time) and the input of the homogeneous transformations (also applied in FPGA), as shown in Fig. 2.

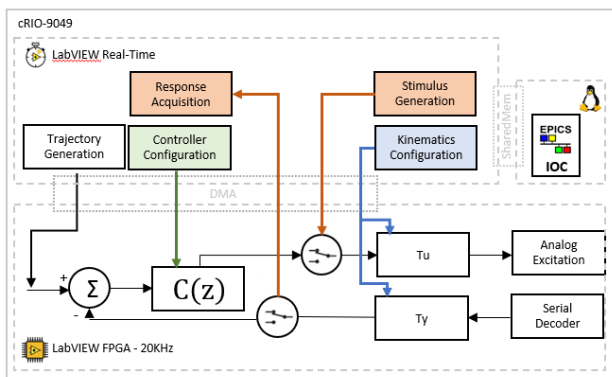

Figure 2: System identification architecture blocks.

When system identification mode is selected, the control algorithm is bypassed by two FIFO buffers where the stimulus signal will be applied in the actuation path and the

* Work supported by the Ministry of Science, Technology and Innovation.
† telles.soares@lnls.br

ISBN: 978-3-95450-238-7 ISSN: 2226-0358 doi:10.18429/JACoW-ICALEPCS2023-TUPDP006

response acquired from the feedback path, both in the same control loop rate.

A detailed architecture of HD-DCM-Lite prototyping control system, which includes the homogeneous transformations, can be found in [6].

STIMULUS GENERATION

There are multiple types of stimulus signal, for instance white noise, chirp, step sine and multi-sine [7] and choosing it accordingly to the physical system is important to achieve a reliable system behavior and accuracy from the estimated model. Multi-sine is broadly applied due to the ability to manipulate each tone or a specific pattern, for example odd or even frequencies. Briefly, the multi sine is a sum of a determined number of sinusoidal components – each one containing a specific frequency and phase, for sine or cosine, the waveform is generated as follow:

$$x(t) = \sum_{k=1}^{N} A_k sin(\omega_k t + \varphi_k) \ . \tag{1}$$

Different methods can be applied to phase the tones in a multi-sine excitation. In other words, there are different ways to choose φ_k. The most usual ways are randomly, linear difference, linear phase and Schröder method [8]. Crest factor and bandpass spectrum are crucial parameters to be considered. The former is the ratio of the peak value to the effective value (RMS) of a waveform. The lower to the theoretical bound, the better the signal stimulus and consequently, the best signal-to-noise ratio (SNR) for the frequency response function of a system behaviour.

Random Phasing

Each phase is chosen randomly (Wichmann-Hill [9]) between 0° and 360°.

Linear Difference

The phase difference between adjacent frequency tones varies linearly from 0° to 360°:

$$\varphi_k = \frac{360k}{N} + \varphi_{k-1} \ . \tag{2}$$

This gives a good Peak/RMS ratio but might cause the signal to have periodic components within the period of the overall waveform.

Linear Phase

The phase varies linearly from 0° to 360°:

$$\varphi_k = \frac{360k}{N} \ . \tag{3}$$

Schröder Phasing

Similar to linear difference, however, Cosine is use instead of Sine, thus tones start at 90°. That provides a better cycle sweeping and bandpass spectrum:

$$\varphi_k = -\frac{\pi k(k-1)}{N} \ . \tag{4}$$

Phasing Methods Comparison

A comparison between the crest factor for all presented methods was performed and used to select the most suited to this application. For a stimulus signal of 10 k samples per second, 0.5 amplitude, 1 Hz start frequency, 1 Hz delta frequency, 4000 tones and 3 cycles (3 seconds) a multitone stimulus was generated and results are shown in Table 1.

Table 1: Crest Factor Comparison

Phase method	Crest factor
Random phasing	3.5 – 5.5
Linear difference	1.9
Linear phasing	64.6
Schröder phasing	1.6

By looking at Table 1, the conclusion is that the phasing based on Schröder method has a better crest factor. So, the decision was to apply this methodology to identify the plants of HD-DCM-Lite and HD-CSS. In addition to the results present in Table 1, the spectrogram of each method can be presented to analyze the spectral density. Figures 3 and 4 show, respectively, the stimulus signal for a single period (1 second) and the spectrogram for all excitation periods (3 seconds) for the random phasing.

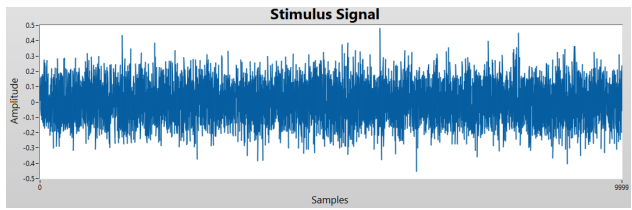

Figure 3: Stimulus signal for a single period (random phasing).

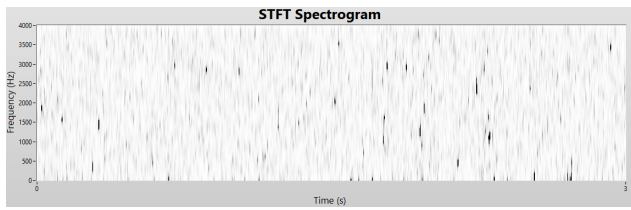

Figure 4: Spectrogram for all periods (random phasing).

Figures 5 and 6 show, respectively, the stimulus signal for a single period (1 second) and the spectrogram for all excitation periods (3 seconds) for the linear difference.

Figures 7 and 8 show, respectively, the stimulus signal for a single period (1 second) and the spectrogram for all excitation periods (3 seconds) for the linear phase.

Figures 9 and 10 show, respectively, the stimulus signal for a single period (1 second) and the spectrogram for all excitation periods (3 seconds) for the Schröder phasing.

Abrupt stimulus in a physical system, considering all the electronic and mechanical subsystems, can be damaging,

ISBN: 978-3-95450-238-7 ISSN: 2226-0358 doi:10.18429/JACoW-ICALEPCS2023-TUPDP006

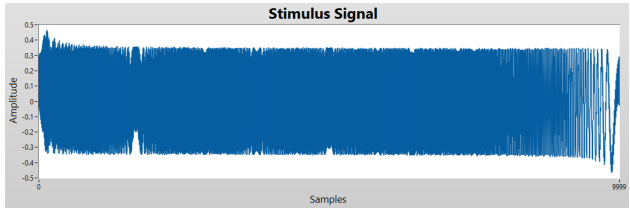

Figure 5: Stimulus signal for a single period (Linear difference).

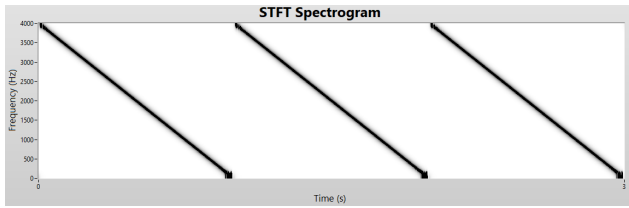

Figure 6: Spectrogram for all periods (Linear difference).

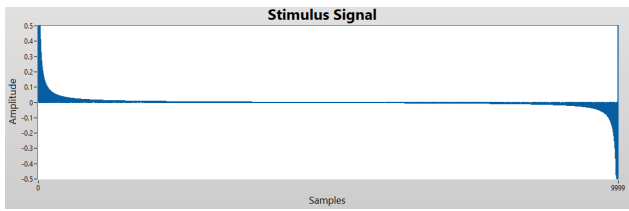

Figure 7: Stimulus signal for a single period (Linear phase).

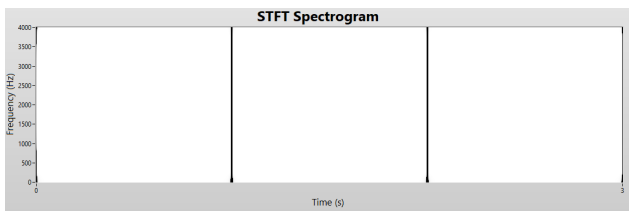

Figure 8: Spectrogram for all periods (Linear phase).

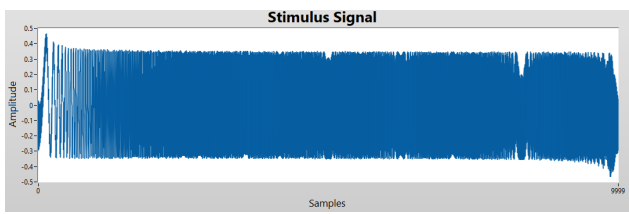

Figure 9: Stimulus signal for a single period (Schröder phase).

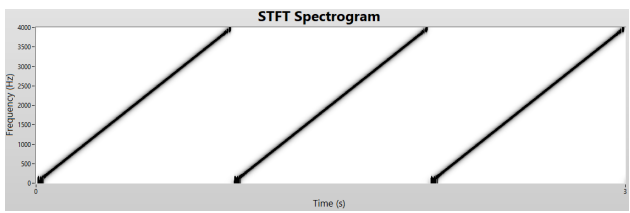

Figure 10: Spectrogram for all periods (Schröder phase).

thus a windowing in the stimulus initial and final amplitude is highly recommended. Similarly, to S curves in a trajectory, Tukey windowing [10] is a good approach to smoothly start and finish a stimulus signal with also the advantage of being very flat within the stimulus region of interest, allowing a seamlessly response data acquisition triggering.

A signal based on Tukey windowing can be built using the following relations:

$$w(t) = \begin{cases} \frac{1}{2}(1 + cos(\frac{2\pi}{r}(x - \frac{r}{2}))), 0 \leq t < \frac{r}{2} \\ 1, \frac{r}{2} \leq t < 1 - \frac{r}{2} \\ \frac{1}{2}(1 + cos(\frac{2\pi}{r}(x - 1 + \frac{r}{2}))), 1 - \frac{r}{2} \leq t \leq 1 \end{cases} . \quad (5)$$

In order to deal with limited SNR and further improve frequency response estimation, the stimulus generator may concatenate a configurable number of periods in the window's flat region, for which system responses are processed separately and averaged together, providing a cleaner frequency response estimation. Figure 11 presents an example of an excitation signal containing 20 periods (or 20 seconds), in which each period has 20 k samples and the data is modulated in 0.015. The first and last 2 seconds are windowed based on Tukey.

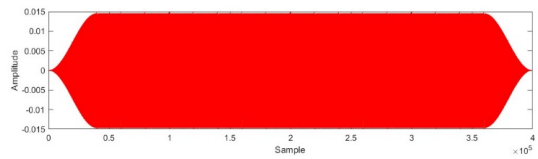

Figure 11: Excitation data with Tukey windowing.

IMPLEMENTATION

For most of application it is not pertinent to dynamically generate the stimulus signal point by point, since it is very resource consuming either for CPU or FPGA due to the number of interactions it requires for every sample. Thereby, the scheme shown in Fig. 12 represents the Stimulus Generations and Response Acquisition blocks. By visualizing this scheme, it is possible to realize that the signal is generated inside the CPU of the cRIO, and then streamed to FPGA using FIFO buffers and a DMA interface. Inside the FPGA, the signal passes by the first homogeneous transformation and then feeds the actuators. Inside the same loop, a feedback signal is read (after passing by the second homogeneous transformation), collected and streamed to CPU using the same methodology based on FIFOs. The two sets of data (excitation and feedback) are then saved in TDMS files to be post-processed by MATLAB – the chosen environment to build Frequency Responses.

SYSTEM IDENTIFICATION: RESULTS

In this section, the system identification procedure involving the post-processing in MATLAB is described. The methodology is to bring the TDMS files – generated after the excitation described in previous sections – into MATLAB and then, build the plants that describe the dynamic

ISBN: 978-3-95450-238-7 ISSN: 2226-0358 doi:10.18429/JACoW-ICALEPCS2023-TUPDP006

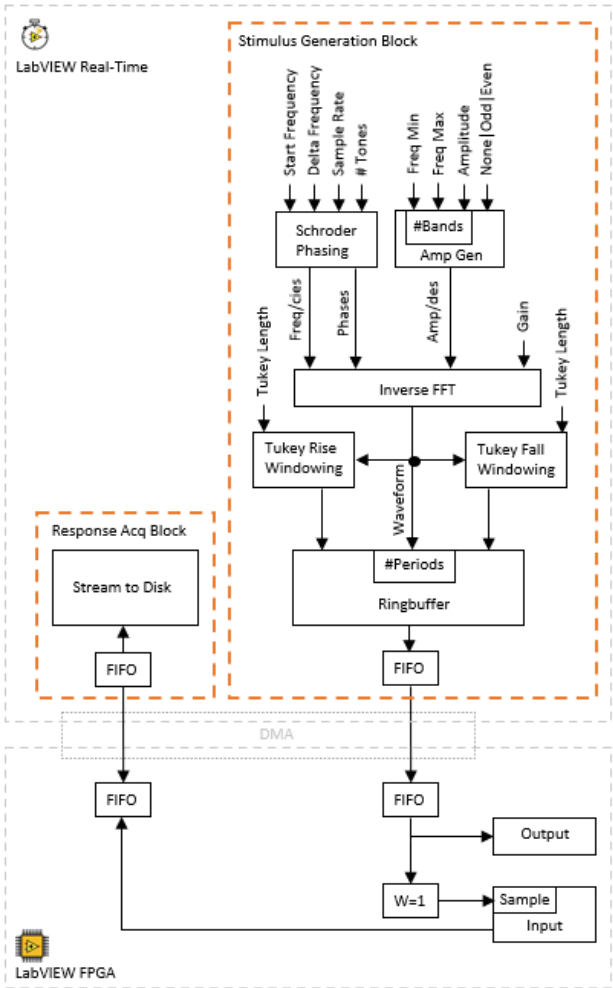

Figure 12: Implementation in LabVIEW to be embedded inside cRIO for system excitation and response acquisition.

behavior of the mechatronic system. Also, the results for HD-DCM-Lite will be shown as well.

Typical Stimulus Signal for HD-DCM-Lite

The typical excitation signals for the high-dynamic monochromator are based on 20 seconds of stimulation (representing 20 periods). In the first and last 2 seconds of stimulus, respectively, the amplitude of excitation modulation increases and decreases. Also, the first and last 4 seconds of the experiment are discarded – and only the 16 remaining periods are used for the system identification. Each one of these 16 remaining periods has a determined Frequency-Response Function (FRF), calculated using the FFT command in MATLAB [11,12]. Then the final FRF of the system is the average of the 16 calculated ones.

It is also important to note that the stimulus signal is modulated to a determined value. This value is found empirically – starts small and, as it grows, the FRF starts to become more defined. Also, the degrees of freedom are stimulated separately. For example: while exciting GAP_u, the other ones (PTC_u and RLL_u) must be held at zero. But in order to calculate the relative gain array (RGA), while exciting GAP_u, all degrees of freedom are acquired and saved – GAP_m, PTC_m and RLL_m. Explanations of what means each degree of freedom mentioned in this section can be found in [6].

Table 2 presents typical characteristics of the multi-sine with Schröder phasing used to excite each degree of freedom from the HD-DCM-Lite. As the excitation and acquisition loop runs at 20 kHz in the FPGA, the maximum excitation tone is 10 kHz.

Table 2: Characteristics of Excitation Data for Short-Stroke System Identification

From	Fmin	Fdelta	Fmax	Mod
GAP_u	1 Hz	1 Hz	10 kHz	0.5 N
PTC_u	1 Hz	1 Hz	10 kHz	0.025 N·m
RLL_u	1 Hz	1 Hz	10 kHz	0.015 N·m

Final Plant for HD-DCM-Lite

The final FRF calculated experimentally following the methodology explained in this paper, for HD-DCM-Lite, is shown in Fig. 13.

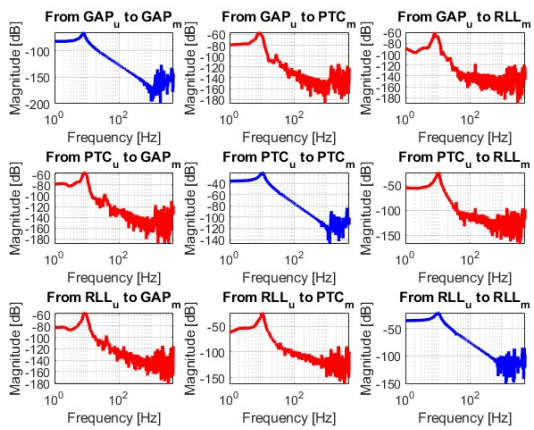

Figure 13: Frequency response obtained experimentally for HD-DCM-Lite (also present in [6]).

CONCLUSION

In [6], it is possible to visualize that the identified plant matched approximately what had been modeled in the mechanical design. The accuracy provided by the comparison between the experimental plant and the dynamic model brings the conclusion that the methodology described in this paper is appropriate for critical mechatronic components and complex control systems in terms of precision engineering, such as HD-DCM-Lite and HD-CSS.

Also, it is important to emphasize that the architecture between Real-Time and FPGA applied several high-performance techniques so that the application is reliable and flexible to other sub-systems across the laboratory.

ISBN: 978-3-95450-238-7 ISSN: 2226-0358 doi:10.18429/JACoW-ICALEPCS2023-TUPDP006

The implementation also brought a quick way to perform diagnosis over the mechatronic system. That is because the prototyping hardware is the same of the final application (cRIO), and so the infrastructure, such as cabling and fibers.

ACKNOWLEDGEMENTS

The authors would like to gratefully acknowledge the funding by the Brazilian Ministry of Science, Technology and Innovation and the contributions of the LNLS team.

REFERENCES

[1] CNPEM, "Sirius: accelerating the future of Brazilian science", https://www.lnls.cnpem.br/sirius-en/

[2] A.V. Perna, G.S. de Albuquerque, H.O.C. Duarte, R.R. Geraldes, M.A.L. Moraes, M. Saveri Silva, and M.S. Souza, "The HD-DCM-Lite: a high dynamic DCM with extended scanning capabilities for Sirius/LNLS beamlines", in *Proc. MEDSI'20*, Chicago, USA, Jul. 2021, pp. 203-206. doi:10.18429/JACoW-MEDSI2020-TUPC11

[3] R.M. Caliari, R.R. Geraldes, M.A.L. Moraes, G.B.Z.L. Moreno, R. Faassen, T.A.M. Ruijl, and R.M. Schneider, "System Identification and Control for the Sirius High-Dynamic DCM", in *Proc. ICALEPCS'17*, Barcelona, Spain, Oct. 2017, pp. 997–1002. doi:10.18429/JACoW-ICALEPCS2017-TUSH203

[4] R.M. Caliari, R.R. Geraldes, M.A.L. Moraes, and G. Witvoet, "Loop-Shaping Controller Design in the Development of the High-Dynamic Double-Crystal Monochromator at Sirius Light Source", *Am. Soc. Precis. Eng. Topical Meetings*, 2020.

[5] National Instruments cRIO-9049, https://www.ni.com/pt-br/shop/model/crio-9049.html

[6] T.R.S. Soares, J.P.S. Furtado, G.S. de Albuquerque, M. Saveri Silva, and R.R. Geraldes, "Dynamical modelling and control development for the new High-Dynamics Double Crystal Monochromator (HD-DCM-Lite) for Sirius/LNLS", presented at ICALEPCS'23, Oct. 2023, Cape Town, South Africa, paper MO2AO07, this conference.

[7] T. Kimpián and F. Augusztinovicz, "Multiphase multisine signals – Theory and practice", in *Proc. 27th Int. Conf. Noise Vib. Eng. (ISMA'16)*, Heverlee, Belgium, Sept. 2016, pp. 2241-2250. https://past.isma-isaac.be/downloads/isma2016/papers/isma2016_0570.pdf

[8] M. Schroeder, "Synthesis of Low-Peak Factor Signals and Binary Sequences with Low Autocorrelation," *IEEE Trans. Inf. Theory*, vol. 16, no. 1, pp. 85-89, Jan. 1970. doi:10.1109/TIT.1970.1054411

[9] Brian A. Wichmann and I. David Hill, "Algorithm AS 183: An Efficient and Portable Pseudo-Random Number Generator", *J. R. Stat. Soc. C*, vol. 31, no. 2, pp. 188–190. doi:10.2307/2347988

[10] J.W. Tukey, "An introduction to the calculations of numerical spectrum analysis", *Spectra Anal. Time*, B. Harris, ed. Wiley: New York, USA, pp. 25–46.

[11] P. Bloomfield, *Fourier Analysis of Time Series: An Introduction*, New York: Wiley-Interscience, 2000.

[12] Fast Fourier transform, https://www.mathworks.com/help/matlab/ref/fft.html